

## High- $\beta$ , improved confinement reversed-field pinch plasmas at high density

M. D. Wyman,<sup>1,a)</sup> B. E. Chapman,<sup>1</sup> J. W. Ahn,<sup>1</sup> A. F. Almagri,<sup>1</sup> J. K. Anderson,<sup>1</sup> F. Bonomo,<sup>2</sup> D. L. Brower,<sup>3</sup> S. K. Combs,<sup>4</sup> D. Craig,<sup>1,5</sup> D. J. Den Hartog,<sup>1</sup> B. H. Deng,<sup>3</sup> W. X. Ding,<sup>3</sup> F. Ebrahimi,<sup>1</sup> D. A. Ennis,<sup>1</sup> G. Fiksel,<sup>1</sup> C. R. Foust,<sup>4</sup> P. Franz,<sup>2</sup> S. Gangadhara,<sup>1</sup> J. A. Goetz,<sup>1</sup> R. O'Connell,<sup>1</sup> S. P. Oliva,<sup>1</sup> S. C. Prager,<sup>1</sup> J. A. Reusch,<sup>1</sup> J. S. Sarff,<sup>1</sup> H. D. Stephens,<sup>1</sup> and T. Yates<sup>3</sup>

<sup>1</sup>Department of Physics, University of Wisconsin–Madison, Madison, Wisconsin 53706, USA

<sup>2</sup>Consorzio RFX, Corso Stati Uniti 4, 35127 Padova, Italy

<sup>3</sup>Department of Physics and Astronomy, University of California at Los Angeles, Los Angeles, California 90095-1594, USA

<sup>4</sup>Oak Ridge National Laboratory, Oak Ridge, Tennessee 37831-8071, USA

<sup>5</sup>Wheaton College, Wheaton, Illinois 60187, USA

(Received 9 November 2007; accepted 20 December 2007; published online 30 January 2008)

In Madison Symmetric Torus [Dexter *et al.*, Fusion Technol. **19**, 131 (1991)] discharges where improved confinement is brought about by modification of the current profile, pellet injection has quadrupled the density, reaching  $n_e = 4 \times 10^{19} \text{ m}^{-3}$ . Without pellet injection, the achievable density in improved confinement discharges had been limited by edge-resonant tearing instability. With pellet injection, the total beta has been increased to 26%, and the energy confinement time is comparable to that at low density. Pressure-driven local interchange and global tearing are predicted to be linearly unstable. Interchange has not yet been observed experimentally, but there is possible evidence of pressure-driven tearing, an instability usually driven by the current gradient in the reversed-field pinch. © 2008 American Institute of Physics. [DOI: 10.1063/1.2835439]

In its standard mode of operation, the ability of the reversed-field pinch (RFP) to confine thermal energy is, typically, relatively poor. This is due to the fact that the internal magnetic field structure is largely stochastic, resulting from the growth and spatial overlap of multiple internally resonant tearing instabilities. The dominant instabilities in the plasma core have poloidal mode number  $m=1$ .<sup>1</sup> These modes are driven primarily by a gradient in the radial profile of the plasma current. One reliable means of reducing these instabilities and improving energy confinement is modification of the current profile via auxiliary inductive current drive.<sup>2</sup> In the Madison Symmetric Torus (MST),<sup>3</sup> discharges where the  $m=1$  and also the edge-resonant  $m=0$  modes are controlled exhibit a tenfold improvement in energy confinement and an approximate doubling of beta, the ratio of plasma pressure to the confining magnetic field pressure.<sup>4,5</sup> This technique has also been successfully applied to other RFP plasmas.<sup>6–8</sup>

The largest improvements in energy confinement and beta have been limited to relatively low density,  $n_e \leq 10^{19} \text{ m}^{-3}$ .<sup>2,4,5,7–11</sup> Above this density in the MST,  $m=0$  instability is triggered, and energy confinement degrades. The only sources of fuel for MST plasmas have been gas puffing and recycling from the plasma-facing wall. It is believed that the  $m=0$  destabilization is due to an unfavorable change in the edge current and/or pressure profiles brought about by the additional flux of cold, neutral particles needed for larger plasma density. In these low-density, ohmically heated plasmas, the reduction of tearing instability resulted in a rapid increase in the electron temperature, while the ion temperature remained unchanged. The maximum electron tempera-

ture (1.3 keV) was as much as four times the ion temperature.<sup>4,5</sup> One mechanism for heating ions is collisional energy transfer from the electrons, but the coupling time  $\sim T_e^{3/2}/n_e$  is ten times longer than the duration of improved confinement. This increase in the electron temperature has led to relatively large  $\beta$ , with total  $\beta$  (defined below) in the MST reaching 15%.<sup>4,5</sup> Although  $\beta$  is high, it is below the threshold for magnetohydrodynamic (MHD) instability. A  $\beta$  limit has yet to be experimentally identified in the RFP.

For the RFP to progress as a fusion reactor concept, improved confinement must be achievable at substantially higher density, and the ion temperature must increase along with the electron temperature. In addition, to better gauge the potential attractiveness of the RFP, the  $\beta$  limit and its cause must be determined.

In this Letter, with the injection of frozen deuterium pellets into discharges with auxiliary current drive, we demonstrate magnetic fluctuation reduction and improved energy confinement with a density reaching  $4 \times 10^{19} \text{ m}^{-3}$ , four times larger than previously possible. We also demonstrate that the ion temperature now increases along with the electron temperature. This has resulted in the highest beta achieved in the improved confinement RFP ( $\beta_{\text{tot}}=26\%$  at 0.2 MA), but this beta does not appear to be the limiting value. The pressure gradient in the core exceeds the Mercier criterion,<sup>12</sup> which locally balances magnetic shear against the pressure gradient, and local interchange instability is predicted to be linearly unstable. However, there is as yet no indication of interchange modes in the experiment, and disruptions are not observed. Pressure-driven tearing is also predicted to be linearly unstable. We do observe that the dominant tearing modes are not reduced to the same degree in these plasmas

<sup>a)</sup>Electronic mail: mwyman@trialphaenergy.com. Present address: Tri Alpha Energy, Rancho Santa Margarita, CA 92688.

as they are at lower density and pressure. Hence, the normally current-gradient-driven tearing instability may now be driven in part by the pressure gradient.

The plasmas described here were produced in the MST, with a plasma minor radius of 0.5 m and a major radius of 1.5 m. In this work, we apply pellet injection to discharges with toroidal plasma currents of 0.2 and 0.5 MA. The pellet injector, built by Oak Ridge National Laboratory, is a pipe gun device<sup>13</sup> consisting of four barrels, in each of which a deuterium pellet is formed and launched. The pellets travel along straight guide tubes aimed at the plasma center, and they enter the plasma 30° poloidally above the outboard mid-plane. The pellets are propelled by high-pressure gas and/or a mechanical punch. The gas-propelled (fast) pellets reach a velocity of ~1200 m/s, while the punch-propelled (slow) pellets reach velocities of 100–200 m/s. Frozen pellet injection has also been applied to other RFPs such as ETA-BETA II,<sup>14</sup> ZT-40M,<sup>15</sup> RFX,<sup>16,17</sup> and TPE-RX.<sup>18</sup> In the case of RFX and TPE-RX, pellet fueling was used in conjunction with auxiliary inductive parallel current drive resulting in transient improvements in energy confinement for RFX and increased densities during improved confinement for TPE-RX.

We achieve the largest density and temperatures at 0.5 MA. Data from a typical pellet-fueled, improved confinement 0.5 MA plasma are shown in Fig. 1. Auxiliary current drive begins at  $t=10$  ms with two 1.6-mm-diam pellets injected shortly thereafter, with velocities of 167 and 1150 m/s. The slower pellet arrives at 10.3 ms, while the faster pellet arrives at 11.4 ms. Both the  $m=0$  and  $m=1$  magnetic fluctuations drop due to the auxiliary current drive. Magnetic fluctuation amplitudes are measured by a toroidal array of magnetic pickup coils at the plasma surface. Shown in Figs. 1(b) and 1(c) are the rms sums of the dominant core-resonant ( $m=1$ ,  $n=8-14$ ) and edge resonant ( $m=0$ ,  $n=1-5$ ) fluctuations, where a cessation of bursts at 14 ms indicates the start of improved confinement, shortly after the ablation of both pellets. Fluctuation reduction at this density has not been possible without pellet injection. A hallmark of previous auxiliary current drive experiments was the rise in electron temperature during improved confinement, usually doubling or tripling, without a concurrent increase in ion temperature.<sup>4</sup> However, as shown in Fig. 1(d), the ion temperature  $T_i(r/a=0.2)$  increases along with the electron temperature during the improved confinement period, which, when considering the higher density, results in a sixfold increase in ion thermal energy. This is believed to be due in part to the order-of-magnitude decrease in the electron-ion coupling time. Of course,  $T_i$  need not necessarily have increased in these plasmas, as ion energy loss could have increased as well. The ion temperature is measured by charge-exchange recombination spectroscopy looking at  $C^{+5}$  ions<sup>19</sup> that are tightly coupled to the bulk deuterons. The electron temperature is measured using soft-x-ray tomography.<sup>20</sup> The drop in  $D_\alpha$  shown in Fig. 1(e) indicates a drop in recycling and in the particle source. There is no gas puffing applied during the time window shown.

Measured with an 11-chord interferometer,<sup>21</sup> the evolution of the electron density profile in an improved confinement discharge with pellet injection is shown in Fig. 2. The

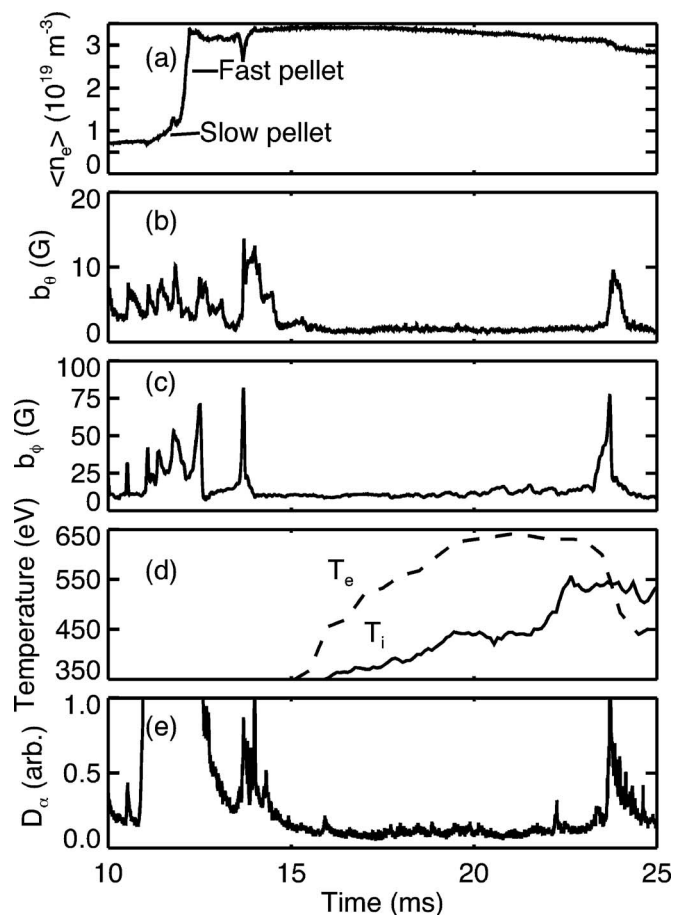


FIG. 1. Waveforms for a 0.5 MA improved confinement discharge with two 1.6-mm-diam pellets injected at roughly 11 ms showing (a) the central line-averaged density, (b) poloidal ( $m=1$ ,  $n=8-14$ ), and (c) toroidal ( $m=0$ ,  $n=1-5$ ) components of magnetic field fluctuations, (d) the electron and ion temperatures at  $r/a=0.2$ , and (e) line emission from neutral deuterium. Auxiliary current drive begins at 10 ms. The delay between arrival time and measured density response is consistent with the time it takes for the pellet to deposit material and for that deposition to affect the local density near the measurement (toroidally displaced 160° from the point of injection). Temperature data before 15 ms are unavailable.

data are from a 0.2 MA plasma in which we achieved the largest beta and which will be further analyzed below, but the profile evolution is the same at 0.5 MA. Improved particle confinement, at low and high current, is implied by the stationary density profile and reduction of  $D_\alpha$  radiation. The global particle confinement time  $\tau_p = N / (\int S dV - dN/dt) < 6$  ms, where  $N = \int n_e dV$ , and  $S$  is the source term, measured using the interferometer and a radial array of  $D_\alpha$  detectors.<sup>22</sup> This is comparable to the value ( $\sim 4.7$  ms) in low-density improved confinement plasmas.<sup>23</sup>

As summarized in Table I, pellet injection and improved confinement lead to a total beta of 17% in high current discharges and 26% at low current, where  $\beta_{\text{tot}} = \langle p \rangle / [B^2(a) / 2\mu_0]$ , and  $\langle p \rangle = \int p dV / \int dV$ , where  $p = n_e T_e + n_i T_i$ . For the calculation of both beta and energy confinement time, electron temperature profiles were measured using a multipoint Thomson scattering diagnostic.<sup>24</sup> Due to the lower electron temperature at high density, the Ohmic input power is greater, and beta is increased. At both high and low

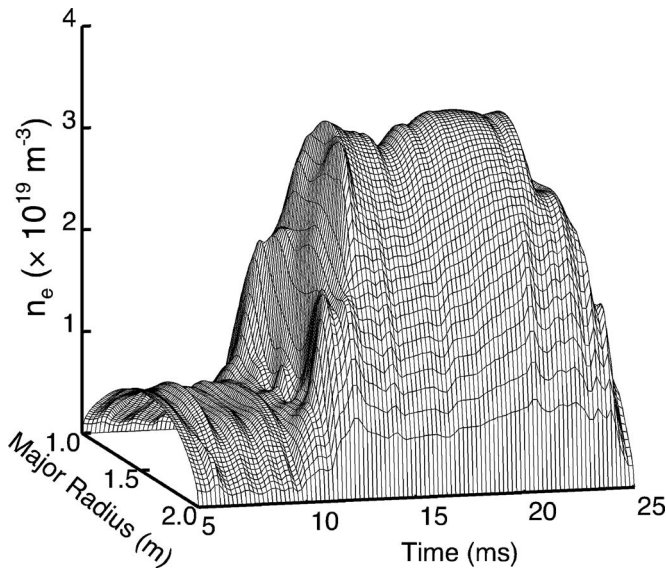


FIG. 2. Electron density profile evolution before and during improved confinement with pellet injection for a 0.2 MA discharge. During  $t = 10$  to 13 ms, a single slow pellet is ablating (only one pellet was injected). Improved confinement begins at 15 ms.

current, the ion component of beta is larger in pellet-fueled discharges.

The energy confinement time is given by  $\tau_E = \int W_{th} dV / \int (P_{oh} - dW_{th}/dt) dV$ , where  $W_{th} = 3/2p$ . In pellet-fueled improved confinement plasmas,  $\tau_E$  exceeds that for standard plasmas (1 ms) and is within a factor of 2 of the best-measured confinement at low density (10 ms). The ohmic input power  $P_{oh}$  is calculated using two methods: from measurements of resistivity and the current profile,  $P_{oh} = \eta J^2$ , and from global power balance,  $P_{oh} = P_{in} - dW_{mag}/dt$ , where the  $P_{in}$  is the input power, and  $W_{mag}$  is the stored magnetic energy. The current and magnetic field profiles are reconstructed using the toroidal equilibrium code MSTFit<sup>25</sup> and are constrained by internal and edge measurements. The neoclassical resistivity is calculated directly from

TABLE I. Plasma parameters, defined in the text (except for poloidal beta,  $\beta_\theta = \langle p \rangle / [B_\theta^2(a) / 2\mu_0]$ ), for discharges with and without pellets and at high and low current. All data were measured during improved confinement at the time of the peak temperature. Low-density data from Ref. 4. Only the central electron temperature was measured in the high- $I_\phi$ , low- $n_e$  case. Energy and particle confinement times in standard plasmas are  $\sim 1$  ms irrespective of current and density.

	Low current		High current	
	Low $n_e$	Pellet-fueled	Low $n_e$	Pellet-fueled
$I_\phi$ (MA)	0.21	0.17	0.50	0.48
$n_e(0)$ ( $10^{19} \text{ m}^{-3}$ )	1.0	3.5	1.0	4.0
$T_e(0)$ (eV)	600	170	1300	700
$T_i(0)$ (eV)	200	190	350	600
$\beta_{tot}$ (%)	15	26	$\sim 6$	17
$\beta_\theta$ (%)	18	40	$\sim 7$	21
$\tau_E$ (ms)	10	5	N/A	7
$\tau_p$ (ms)	4.7	4.3	N/A	5.5

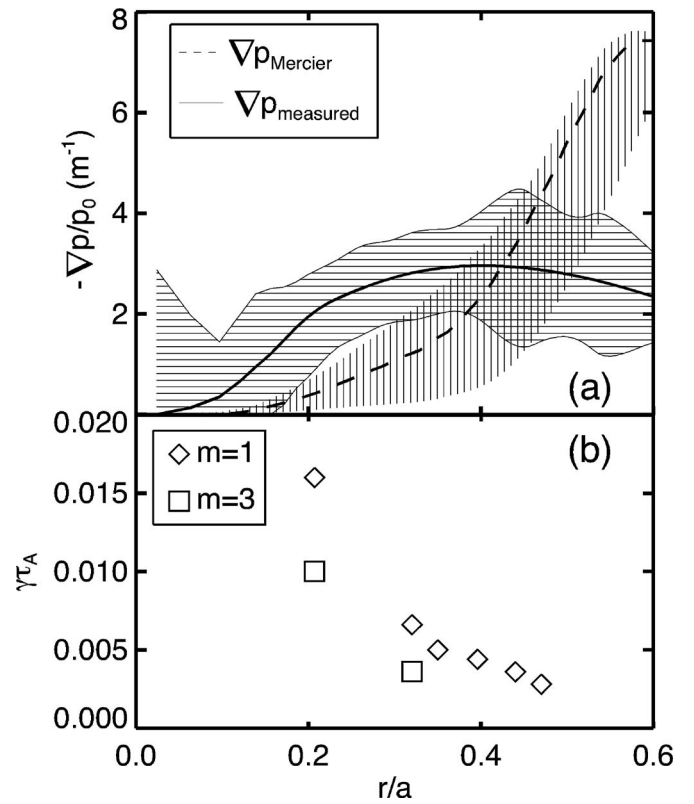


FIG. 3. Pressure gradient profiles and calculated growth rates of pressure driven modes. The pressure gradient profile for a low current, pellet fueled discharge is plotted with the associated Mercier limit [ $\nabla p_{\text{Mercier}} = -rB_\theta^2 / (32\pi)(q'/q)^2 / (1-q^2)$ ] in (a). For the critical pressure gradient,  $B_\theta$  is the toroidal field,  $q$  is the safety factor, and  $q' = dq/dr$ . In (b) the calculated growth rates for  $m=1$  and  $m=3$  modes are plotted vs resonance location with  $\tau_A \sim 1 \mu\text{s}$ . All modes are resistive and pressure driven.

measurements of  $T_e$  and  $Z_{\text{eff}}$ .  $Z_{\text{eff}}$  is measured in 0.5 MA discharges to increase from 2.1 to 2.9 during improved confinement. For the high current case, the two methods yield an energy confinement time of 7 ms. The confinement time at low current is estimated to be 5 ms, calculated with  $Z_{\text{eff}}$  assumed to be 2, limited measurements of the current profile, and without measurement of the  $dT/dt$  term in  $dW_{th}/dt$ .

At high beta, the pressure gradient is expected to become a larger source of energy for instability. At low  $I_p$  (0.2 MA), the pressure gradient during pellet-fueled discharges exceeds the Mercier criterion<sup>12</sup> inside of  $r/a=0.4$  [Fig. 3(a)]. Past experimental work in the stellarator has shown that exceeding the Mercier criterion does not result in deleterious instability.<sup>26</sup> However, this is the first instance of the pressure gradient exceeding the Mercier criterion in the RFP, confirming recent theoretical work predicting that the criterion would not represent a fundamental limit for the RFP.<sup>27</sup> Linear resistive MHD stability calculations predict that localized, Mercier-like (high- $n$ ) interchange modes resonant in the core are unstable with growth times  $\leq 200 \mu\text{s}$ , as shown in Fig. 3(b) for  $m=3$  modes. Although instabilities are predicted, we do not observe any effects that would be endemic to interchange activity, e.g., flattening of the pressure profile, indicating that either the modes are saturated at low amplitude or that the spatial scale of any effect is smaller than we can resolve.

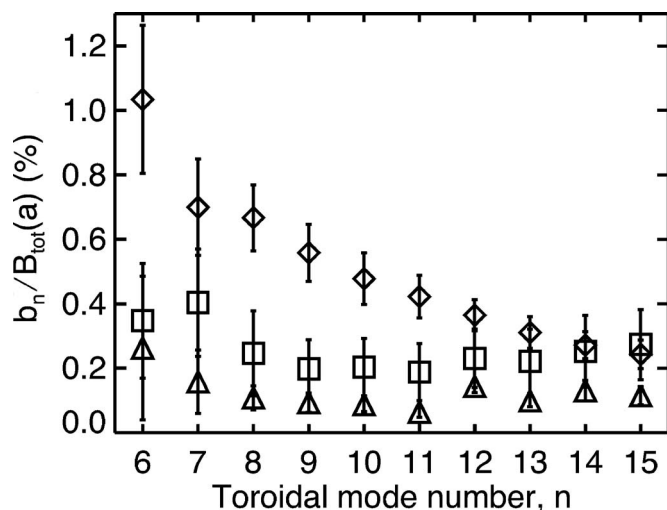


FIG. 4. Magnetic fluctuation spectra for three different operating regimes: (◇) standard confinement at low density, (△) improved confinement at low density, and (□) improved confinement at high density via pellet fueling.

The stability calculation also predicts growing global ( $m=1$ ) pressure-driven tearing modes [Fig. 3(b)]. This represents a new regime for RFP plasmas. In standard confinement discharges, tearing modes are present but are driven by the current gradient. In low-density improved confinement discharges, these modes are predicted to be linearly stable to both the current and pressure gradients. The modes are also linearly stable to the current gradient in high-density improved confinement plasmas. Comparison of the experimental  $m=1$  magnetic fluctuation spectra (Fig. 4) for these three regimes shows the reduction with auxiliary inductive current drive, at both low and high density. However, the reduction is smaller at high density, which may be a result of the higher pressure. This smaller reduction may also account for the smaller improved energy confinement time. Although pressure may be playing a larger role in these plasmas, a pressure-driven  $\beta$  limit has apparently not yet been reached.

In summary, we have shown that substantially improved confinement is now possible at high density through the injection of deuterium pellets into discharges with auxiliary current drive. Magnetic fluctuations remain low, limiting fluctuation-induced transport of particles and energy. The increase in density leads to better thermal coupling of ions and electrons, and for the first time, an increasing ion temperature has been observed during improved confinement, resulting in a substantial increase in ion thermal energy. The energy confinement time at high current is improved up to sevenfold over the standard value and is comparable to that of low-density improved confinement plasmas. At low current, pellet injection has led to a record  $\beta_{\text{tot}}=26\%$  for improved confinement RFP plasmas. Local interchange and

global tearing modes are linearly unstable. Interchange has not yet been observed experimentally, but there is possible evidence of pressure-driven tearing.

This work is supported by the U.S. Department of Energy.

- <sup>1</sup>H. Bodin and A. Newton, Nucl. Fusion **20**, 1255 (1980).
- <sup>2</sup>J. S. Sarff, S. A. Hokin, H. Ji, S. C. Prager, and C. R. Sovinec, Phys. Rev. Lett. **72**, 3670 (1994).
- <sup>3</sup>R. N. Dexter, D. W. Kerst, T. W. Lovell, S. C. Prager, and J. C. Sprott, Fusion Technol. **19**, 131 (1991).
- <sup>4</sup>B. E. Chapman, A. F. Almagri, J. K. Anderson *et al.*, Phys. Plasmas **9**, 2061 (2002).
- <sup>5</sup>B. E. Chapman, J. K. Anderson, T. M. Biewer *et al.*, Phys. Rev. Lett. **87**, 205001 (2001).
- <sup>6</sup>R. Bartiromo, P. Martin, S. Martini, T. Bolzonella, A. Canton, P. Innocente, L. Marrelli, A. Murari, and R. Pasqualotto, Phys. Rev. Lett. **82**, 1462 (1999).
- <sup>7</sup>M. Cecconello, J.-A. Malmberg, G. Spizzo, B. E. Chapman, R. M. Gravesstijn, P. Franz, P. Piovesan, P. Martin, and J. R. Drake, Plasma Phys. Controlled Fusion **46**, 145 (2004).
- <sup>8</sup>Y. Yagi, Y. Maejima, H. Sakakita, Y. Hirano, H. Koguchi, T. Shimada, and S. Sekine, Plasma Phys. Controlled Fusion **44**, 335 (2002).
- <sup>9</sup>J. S. Sarff, A. F. Almagri, M. Cecik *et al.*, Phys. Plasmas **2**, 2440 (1995).
- <sup>10</sup>J. S. Sarff, N. E. Lanier, S. C. Prager, and M. R. Stoneking, Phys. Rev. Lett. **78**, 62 (1997).
- <sup>11</sup>M. R. Stoneking, N. E. Lanier, S. C. Prager, J. S. Sarff, and D. Sinityn, Phys. Plasmas **4**, 1632 (1997).
- <sup>12</sup>C. Mercier, Nucl. Fusion Suppl. **2**, 801 (1962).
- <sup>13</sup>S. K. Combs, L. R. Baylor, D. T. Fehling *et al.*, Fusion Sci. Technol. **44**, 513 (2003).
- <sup>14</sup>V. Antoni, A. Buffa, L. Carraro *et al.*, Plasma Phys. Controlled Nucl. Fusion Res. **2**, 441 (1987).
- <sup>15</sup>G. A. Wurden, P. G. Weber, R. G. Watt, C. P. Munson, J. C. Ingraham, R. B. Howell, T. E. Cayton, K. Buchl, and E. J. Nilles, Nucl. Fusion **27**, 857 (1987).
- <sup>16</sup>R. Bartiromo, A. Buffa, V. Antoni *et al.*, Nucl. Fusion **39**, 1697 (1999).
- <sup>17</sup>R. Lorenzini, L. Garzotti, B. Pégourié, P. Innocente, and S. Martini, Plasma Phys. Controlled Fusion **44**, 233 (2002).
- <sup>18</sup>H. Koguchi, D. Terranova, P. Innocente, R. Lorenzini, H. Sakakita, T. Asai, Y. Yagi, Y. Hirano, and K. Yambe, Jpn. J. Appl. Phys., Part 2 **45**, L1124 (2006).
- <sup>19</sup>D. J. Den Hartog, D. Craig, D. A. Ennis *et al.*, Rev. Sci. Instrum. **77**, 122 (2006).
- <sup>20</sup>P. Franz, F. Bonomo, G. Gadani, L. Marrelli, P. Martin, P. Piovesan, G. Spizzo, B. E. Chapman, and M. Reyfman, Rev. Sci. Instrum. **75**, 4013 (2004).
- <sup>21</sup>D. L. Brower, Y. Jiang, W. X. Ding, S. D. Terry, N. E. Lanier, J. K. Anderson, C. B. Forest, and D. Holly, Rev. Sci. Instrum. **72**, 1077 (2001).
- <sup>22</sup>J. K. Anderson, P. L. Andrew, B. E. Chapman, D. Craig, and D. J. Den Hartog, Rev. Sci. Instrum. **74**, 2107 (2003).
- <sup>23</sup>N. E. Lanier, D. Craig, J. K. Anderson, T. M. Biewer, B. E. Chapman, D. J. Den Hartog, C. B. Forest, S. C. Prager, D. L. Brower, and Y. Jiang, Phys. Rev. Lett. **85**, 2120 (2000).
- <sup>24</sup>H. Cummings, J. A. Reusch, R. O'Connell, and D. J. Den Hartog, Bull. Am. Phys. Soc. **50**, 37 (2005).
- <sup>25</sup>J. Anderson, C. Forest, T. Biewer, J. Sarff, and J. Wright, Nucl. Fusion **44**, 162 (2004).
- <sup>26</sup>S. Okamura, K. Matsuoka, K. Nishimura *et al.*, Plasma Phys. Controlled Nucl. Fusion Res. **1**, 381 (1994).
- <sup>27</sup>F. Ebrahimi, S. C. Prager, and C. R. Sovinec, Phys. Plasmas **9**, 2470 (2002).